First-principles study of the electronic structure and exchange interactions in bcc europium

I. Turek,[1,2,*] J. Kudrnovský,[3] M. Diviš,[2] P. Franek,[2] G. Bihlmayer,[4] and S. Blügel[4,5]
[1]*Institute of Physics of Materials, Academy of Sciences of the Czech Republic, Žižkova 22, CZ-61662 Brno, Czech Republic*
[2]*Department of Electronic Structures, Charles University in Prague, Ke Karlovu 5, CZ-12116 Prague 2, Czech Republic*
[3]*Institute of Physics, Academy of Sciences of the Czech Republic, Na Slovance 2, CZ-18221 Prague 8, Czech Republic*
[4]*Institut für Festkörperforschung, Forschungszentrum Jülich, D-52425 Jülich, Germany*
[5]*Fachbereich Physik, Universität Osnabrück, D-49069 Osnabrück, Germany*
(Received 22 September 2002; revised manuscript received 6 October 2003; published 29 December 2003)

Magnetic properties of the europium metal in a bcc structure are studied from first principles using a two-step approach. First, the electronic structure of a ferromagnetic state is calculated in the local spin-density approximation (LSDA) to the density-functional theory whereby the highly localized $4f$ orbitals are treated as part of the atomic core. This description leads to an equilibrium lattice constant that compares well with experiment, in contrast to the standard LSDA which yields a significantly smaller atomic volume. In the second step, parameters of an effective Heisenberg Hamiltonian are derived from the self-consistent electronic structure and they are used to determine the magnetic ground state and to estimate the magnetic transition temperature. The calculated pairwise exchange interactions tend to couple the local magnetic moments of the nearest neighbors ferromagnetically. However, the interaction parameters exhibit a slow oscillatory decay as a function of the interatomic distance which makes them fully compatible with an observed spin-spiral ground state. The resulting wave vector of the spiral as well as the Néel temperature are in fair agreement with measured values.

DOI: 10.1103/PhysRevB.68.224431 PACS number(s): 75.10.Hk, 71.27.+a

I. INTRODUCTION

Electronic and magnetic properties of rare-earth (RE) metals and RE-based alloys represent a long-standing challenge for first-principles theory of solids. While a general exact formalism is provided by the density-functional theory[1,2] (DFT), standard approximations to the DFT like the local spin-density approximation[3,4] (LSDA) and the generalized gradient approximation[5] (GGA) fail in a reliable treatment of ground-state properties of these systems due to highly localized $4f$ electrons. A simple tool improving the situation in a number of cases is an ''open-core'' approach:[6] the localized $4f$ orbitals are not contained in the valence basis set but are treated as part of the atomiclike core. This idea was often employed in self-consistent spin-polarized calculations of RE-based systems during the last decade[7–9] but its origin dates back to non-self-consistent calculations of a paramagnetic state.[10,11] More sophisticated methods include a LDA+U scheme[12] and the self-interaction corrected (SIC) LSDA approach.[6,13] Ground-state magnetic structures of $4f$ electron systems are often noncollinear and incommensurate with the underlying chemical unit cell[14] which presents another complication for *ab initio* techniques. Consequently, most of the existing calculations were performed for collinear spin structures, both for elementary RE metals[13] and for their alloys, especially with transition $3d$ metals,[6] whereas noncollinear structures have been calculated only very recently.[15,16]

Generalizations of the DFT to finite temperatures and excited states are possible, at least in principle. On a practical level, however, additional assumptions and approximations are inevitable for a treatment of finite-temperature properties and magnetic excitations. A substantial progress in magnetic $3d$ transition metals and alloys has been achieved by employing the local magnetic moments as classical degrees of freedom relevant for spin dynamics and statistical physics. This concept can be justified by an adiabatic approximation[17,18] and it can be applied in different ways. One way is to describe the paramagnetic state in terms of the so-called disordered-local-moment (DLM) picture and to derive the magnetic transition temperature from a linear-response theory.[17,19] Another possibility is to consider a collinear magnetic state and to map the total energy changes accompanying small deviations of the local moment directions onto a classical pairwise Heisenberg Hamiltonian[18,20,21] which serves as a starting point for evaluation of magnon spectra, spin-wave stiffness constants, magnetic phase diagrams, etc. Both approaches are quite successful for metals with large moments (Fe) whereas difficulties are encountered for systems with small moments (Ni). For RE metals a theory based on intraatomic exchange integrals has been derived within the LSDA (Ref. 22) which, however, failed to describe quantitatively the Curie temperature of ferromagnetic gadolinium. For RE-based alloys containing $3d$ transition metals, a mapping of the total energies calculated for different spin configurations onto a Heisenberg Hamiltonian was considered as well, but systematic studies of the Curie temperatures are still missing, see Ref. 6 and references therein.

Europium is a RE metal with half-filled $4f$ level. Its equilibrium crystal structure is body-centered-cubic (bcc) with a lattice constant ranging from $a=4.582$ Å at room temperature to $a=4.555$ Å for temperatures below 100 K.[23] The magnetic ground state is a spin spiral and the Néel temperature amounts to 91 K.[23,24] Eu in the bcc structure exhibits an anomalously large atomic volume[13,14] related directly to its divalent state and it is thus well suited for testing various *ab initio* schemes. The aim of this article is to apply a simple

two-step procedure to selected properties of bcc Eu. First, the zero-temperature electronic structure of Eu in a ferromagnetic (FM) state is calculated in the standard DFT (LSDA, GGA) as well as in the open-core treatment. The latter yields an equilibrium lattice constant in good agreement with experiment. In the second step, an effective Heisenberg Hamiltonian is constructed and used in searching the magnetic ground state and calculating the transition temperature. It can be expected that this approach is appropriate for Eu with big local magnetic moments due to the half-filled $4f$ level. We find that the experimentally observed spin spiral arises due to a long-range character of the exchange interactions which is caused by the Ruderman-Kittel-Kasuya-Yoshida (RKKY) mechanism analogous to that encountered in $3d$ transition metals[21] and that the measured Néel temperature can be roughly reproduced within the present scheme.

II. FORMALISM AND COMPUTATIONAL DETAILS

Most of the results reported here are based on self-consistent LSDA calculations using the all-electron scalar-relativistic tight-binding linear muffin-tin orbital (TB-LMTO) method in the atomic-sphere approximation (ASA).[25,26] The exchange-correlation potential was parametrized according to Ref. 27 and the Brillouin-zone (BZ) integrals were replaced by sums over 1938 **k** points in the irreducible wedge of the BZ. As the position of the (occupied) majority $4f$ orbitals is very close to the Fermi energy, their description as true core states, necessary in the open-core treatment, is impossible and a modified boundary condition to the single-site eigenvalue problem has to be supplied. We decided to take it as $D_\ell(E)=-\ell-1$, where $\ell=3$ and $D_\ell(E)$ denotes the logarithmic derivative of the solution to the radial Schrödinger equation at the atomic-sphere boundary. The eigenvalue coincides then with the center of a pure (unhybridized) ℓ band of the LMTO-ASA method[28] and its contribution to the total energy is thus consistent with neglected hybridization of the $4f$ orbitals with the rest of the valence basis. The same boundary condition has recently been used in a systematic study of the heavy RE's Gd through Tm.[9]

For the sake of comparison, the Kohn-Sham equations of the LSDA and GGA were also solved using the full potential linearized augmented plane-wave (FLAPW) method[29] as implemented in the WIEN[30] and FLEUR[31] codes. The latter implementation enables us to perform also LDA+U and GGA+U calculations, including optionally noncollinear spin structures as well. A detailed account of the results will be published elsewhere.[16]

The effective Heisenberg Hamiltonian constructed in this paper is given by

$$H_{\mathrm{eff}}=-\sum_{\mathbf{RR}'} J_{\mathbf{RR}'}\mathbf{e}_{\mathbf{R}}\cdot\mathbf{e}_{\mathbf{R}'}, \tag{1}$$

where the subscript **R** labels the lattice sites, the vectors $\mathbf{e}_{\mathbf{R}}$ are unit vectors pointing in the direction of the individual local moments, and the pair exchange interactions $J_{\mathbf{RR}'}$ satisfy $J_{\mathbf{RR}'}=J_{\mathbf{R}'\mathbf{R}}$ and $J_{\mathbf{RR}}=0$. They can be calculated using the magnetic force theorem[20,32] applied within the TB-LMTO-ASA method:[21]

$$J_{\mathbf{RR}'}=-\frac{1}{8\pi i}\int_C \mathrm{tr}_L[\Delta_{\mathbf{R}}(z)g^{\uparrow}_{\mathbf{RR}'}(z)\Delta_{\mathbf{R}'}(z)g^{\downarrow}_{\mathbf{R}'\mathbf{R}}(z)]dz. \tag{2}$$

In Eq. (2), the symbol tr_L denotes the trace over the angular momentum index $L=(\ell m)$ and energy integration is performed in the complex energy plane along a closed contour C starting and ending at the Fermi energy (with the occupied part of the valence band lying inside C). The quantities $g^{\sigma}_{\mathbf{RR}'}(z)$ (σ being a spin index, $\sigma=\uparrow,\downarrow$) denote site-off-diagonal blocks of the so-called auxiliary Green-function matrices with elements $g^{\sigma}_{\mathbf{R}L,\mathbf{R}'L'}(z)$ while $\Delta_{\mathbf{R}}(z)=P^{\uparrow}_{\mathbf{R}}(z)-P^{\downarrow}_{\mathbf{R}}(z)$ are diagonal matrices related to the potential functions $P^{\sigma}_{\mathbf{R}}\ell(z)$ of the TB-LMTO-ASA method.[26] The parameters $J_{\mathbf{RR}'}$ determined by Eq. (2) do not contain contributions due to constraining magnetic fields necessary to keep a frozen noncollinear spin structure a stationary state of the Kohn-Sham equation. We believe that due to the large magnetic moment of Eu and the small dependence of the moment magnitude upon rotations (see below), these contributions can be neglected. Reliable evaluation of the exchange interactions $J_{\mathbf{RR}'}$ for distances $d=|\mathbf{R}-\mathbf{R}'|$ up to ten lattice constants was achieved by using 4×10^6 **k** points in the full BZ averages defining the site-off-diagonal blocks $g^{\sigma}_{\mathbf{RR}'}(z)$.[26] More details can be found in Ref. 21.

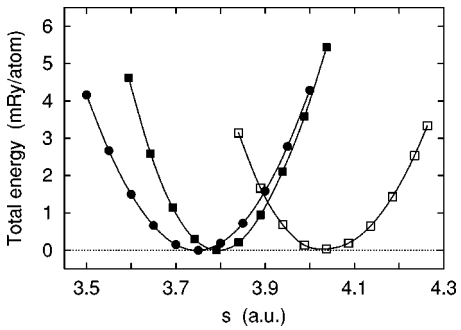

FIG. 1. Total energy of bcc Eu in the FM state as a function of the Wigner-Seitz radius s for different schemes and techniques: LSDA/TB-LMTO-ASA (full circles), LSDA/FLAPW (full squares), and GGA/FLAPW (open squares). The data were shifted to a common reference energy.

III. RESULTS

A. Electronic structure and cohesive properties

Let us discuss first the results of standard LSDA (or GGA) calculations focused on the equilibrium lattice constant in the FM state of bcc Eu. The total energy as a function of the Wigner-Seitz radius s is shown in Fig. 1 for the FLAPW[30] and the ASA techniques. One can see that both LSDA calculations yield an equilibrium Wigner-Seitz radius that is about 11% smaller than the low-temperature experi-

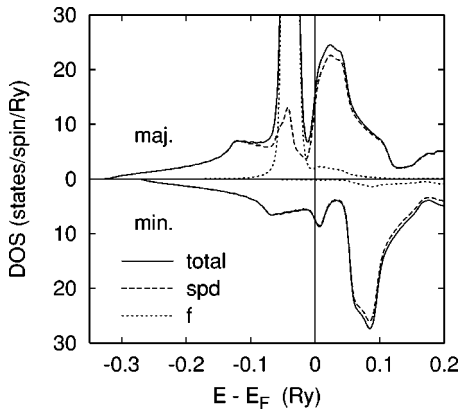

FIG. 2. Spin-polarized DOS for bcc Eu in FM state (LSDA, $s=4.19$ a.u., TB-LMTO-ASA): total (full lines), *spd* projected (dashed), and *f* projected (dotted).

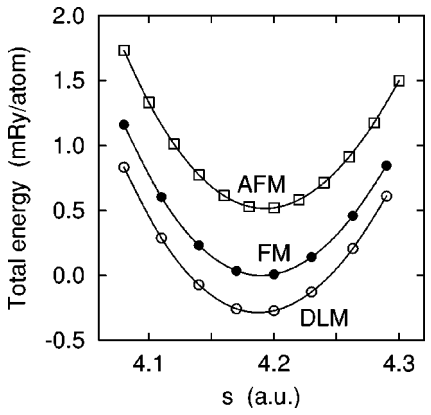

FIG. 3. Total energy of bcc Eu for different spin structures as functions of the Wigner-Seitz radius *s* in the open-core treatment (TB-LMTO-ASA). The zero on the energy scale was set to the minimum for the FM state.

mental one, $s_{expt}=4.238$ a.u. (1 a.u.$=0.529$ Å). The GGA leads to an expansion of the lattice to an equilibrium radius *s* about 5% smaller than s_{expt}.

The origin of the ''overbinding'' is clearly identified looking at the spin-polarized density of states (DOS) decomposed into *spd* and *f* contributions, see Fig. 2. The majority $4f$ orbitals are nearly fully occupied but they are close to the Fermi energy so that a non-negligible tail of the *f*-projected DOS contributes to the bonding and to a strong reduction of the atomic volume. It should be noted that a similar tail is encountered in the minority *f* states in LSDA results of gadolinium.[31] Its influence on the equilibrium atomic volume in the Gd case is less pronounced as compared to Eu but it affects simultaneously the stability of the FM Gd state in favor of an antiferromagnetic (AFM) spin structure.[31,33,34] The calculated numbers of Eu $4f$ electrons for $s=4.0$ a.u. amount to $N_{4f}^{\uparrow}=6.801$, $N_{4f}^{\downarrow}=0.011$ in the LMTO-ASA method, and to $N_{4f}^{\uparrow}=6.692$, $N_{4f}^{\downarrow}=0.002$ in the FLAPW method[30] (the latter numbers refer to a smaller radius of the muffin-tin sphere used, $r_{MT}=2.65$ a.u.). These values do not change substantially over the interval of lattice constants studied.

The effect of $4f$ electrons on the Eu equilibrium lattice parameter should not be confused with the well-known LSDA overbinding,[35] which would already have been (at least partially) reduced by using the GGA. But even a GGA calculation yields a lattice parameter that is 5% too small, i.e., far outside the typical GGA errors. A more detailed analysis for an analogous case of $5f$ electrons in the actinides was given in Ref. 36.

Let us turn to the open-core treatment. On the basis of the previous LSDA calculations, one can fix the occupation of the majority atomiclike $4f$ level at seven electrons leaving the minority counterpart empty. The calculated energy-volume dependence is shown in Fig. 3 for three different spin structures: the FM state, the DLM state and an AFM state. The DLM state with moments pointing in random directions was handled in the coherent-potential approximation[17,26] (CPA) while the AFM state on the bcc lattice was assumed in the CsCl arrangement. The BZ integration for the AFM state employed 2024 **k** points in the irreducible BZ of the CsCl structure. We note that the isotropic DLM state treated within the CPA reduces to a compensated collinear random binary alloy containing 50% positive and 50% negative moments.[17] The marked improvement regarding the equilibrium lattice constant due to the open-core description is clearly seen: the relative deviation of the calculated equilibrium atomic-sphere radius *s* ($s\approx 4.19$ a.u.) with respect to experiment ($s_{expt}=4.238$ a.u.) is merely -1.1%, irrespective of the spin structure.

It should be noted that the equilibrium lattice constant is quite sensitive to the choice of the single-site boundary condition: the $4f$ eigenvalue satisfying the condition modified, e.g., to $D_{\ell}(E)=-\ell=-3$, leads to an equilibrium Wigner-Seitz radius $s\approx 4.12$ a.u., i.e., 2.7% below the experiment. This value is still substantially closer to the experiment than the original LSDA value, but the non-negligible sensitivity of the equilibrium atomic volume to the logarithmic derivative at the sphere boundary represents an unpleasant feature of the open-core treatment.

The calculated energy differences among the three spin arrangements are rather small being of the correct order of magnitude (≈ 1 mRy/atom) as compared to the experimental Néel temperature (91 K, 1 mRy$\equiv$158 K). Interestingly, the FM state is stable with respect to the simple AFM state but both collinear spin structures lie higher in energy than the DLM state. With a neglect of additional inaccuracy due to the CPA employed in the DLM calculations, Fig. 3 indicates a tendency to a more complicated magnetic ground state.

In view of the small calculated energy differences (Fig. 3), the convergence behavior of the ground-state properties with respect to the number of **k** points has to be checked carefully. We have repeated the calculations using the CsCl unit cell for each of the three spin structures (FM, AFM, DLM), eliminating thus any possible source of error due to different BZ. The irreducible part of the BZ has been sampled with a finer mesh of 5984 **k** points. The resulting equilibrium Wigner-Seitz radii deviate from the previous ones less than 0.001 a.u. while the equilibrium total energies as well as their differences deviate less than 0.01 mRy/atom. This proves reliability of our ground-state calculations.

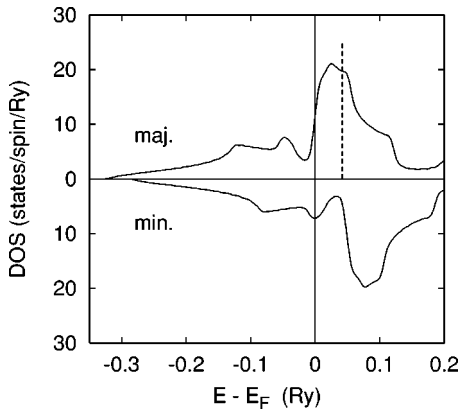

FIG. 4. Spin-polarized DOS for bcc Eu in FM state (open core, $s=4.19$ a.u., TB-LMTO-ASA). The dashed vertical line marks the position of the occupied $4f$ level.

The DOS for the theoretical equilibrium lattice parameter is shown in Fig. 4. A comparison of the profiles in Fig. 4 and the *spd* contributions in Fig. 2 reveal a little sensitivity of the *spd*-projected DOS's with respect to treatment of $4f$ orbitals. The DOS's obtained in the FLAPW technique[30] are very similar to the TB-LMTO-ASA ones, both in the standard LSDA and in the open-core treatment.

The resulting position of the majority core $4f$ level slightly above the Fermi energy (Fig. 4) illustrates a well-known internal inconsistency of the open-core treatment:[6,8] fixing the $4f$ occupation number to an integer value often violates the Kohn-Sham rule to occupy the lowest one-electron states in constructing the charge and spin density. Since a qualitatively similar situation was encountered using both FLAPW techniques,[30,31] we have not tried to remedy this failure by changing the single-site boundary condition.

It should be mentioned that switching from the LSDA and GGA (with $4f$ orbitals in the valence basis) to LDA+U and GGA+U within the FLAPW technique[31] expands the lattice constant, respectively, to -5.3% and $+0.2\%$ (relative deviations from the room-temperature experimental value).[16] The underlying mechanism is essentially the same, namely a removal of the $4f$ orbitals from the vicinity of the Fermi energy. It has been shown for gadolinium that both LDA+U and an open-core treatment represent from this point of view equivalent modifications of the LSDA.[31] But while in Gd the minority $4f$ states are completely unoccupied, both in the open-core and the LDA+U treatment, in the Eu case the majority $4f$ electrons are still in the valence-band region. Their presence accounts for the rather large difference in the calculated lattice parameters (5.3% too small in LDA+U, while a FLAPW open-core calculation gives only a 2.5% too small value).

The resulting Eu magnetic moments depend slightly on the particular scheme employed. For the FM state and the Wigner-Seitz radius $s=4.19$ a.u., the standard LSDA (with $4f$ orbitals in the valence basis) leads to $M=7.30\ \mu_B$ while the open-core treatment yields $M=7.25\ \mu_B$ (both values in the TB-LMTO-ASA method). The dependence of the local moment magnitude on the spin structure was studied within the open-core scheme. For the same Wigner-Seitz radius, the local moments in the AFM and DLM states amount to $M=7.11\ \mu_B$ and $M=7.21\ \mu_B$, respectively. These values prove the changes in *spd* valence bands due to different spin arrangements. However, the relative differences are rather small with respect to the big magnitude of the moment itself which is a necessary prerequisite for reliable applicability of the classical Heisenberg Hamiltonian.

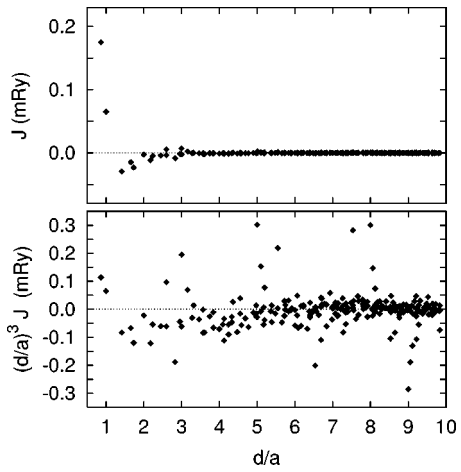

FIG. 5. Exchange interactions $J_{\mathbf{RR}'}$ for bcc Eu as a function of the interatomic distance $d=|\mathbf{R}-\mathbf{R}'|$: without (top panel) and with (bottom panel) a prefactor d^3.

B. Exchange interactions

The parameters $J_{\mathbf{RR}'}$ of the Heisenberg Hamiltonian, calculated in the FM state with the theoretical equilibrium Wigner-Seitz radius $s=4.19$ a.u., are shown in the top panel of Fig. 5. The first nearest-neighbor interactions dominate while the magnitude of the interactions of more distant pairs decays rapidly with increasing distance $d=|\mathbf{R}-\mathbf{R}'|$. A detailed theoretical analysis[21] of the asymptotic behavior of $J_{\mathbf{RR}'}$ along a fixed direction of the vector $\mathbf{R}-\mathbf{R}'$ reveals an RKKY-like oscillatory dependence containing terms the amplitude of which decays proportionally to d^{-3}. The calculated data—though probably in a preasymptotic region—are roughly consistent with this picture, as illustrated by the bottom panel of Fig. 5: interactions of both positive and negative signs are present with an envelope decaying like d^{-3}.

The RKKY asymptotics has profound influence on those properties that are expressed as real-space sums involving the parameters $J_{\mathbf{RR}'}$. This refers, e.g., to the lattice Fourier transform of the exchange interactions defined by

$$J(\mathbf{q})=\sum_{\mathbf{R}} J_{\mathbf{0R}}\exp(\mathrm{i}\mathbf{q}\cdot\mathbf{R}), \tag{3}$$

where $\mathbf{q}$ denotes a vector in the BZ. The convergence property of Eq. (3) for a parameter $J_0\equiv J(\mathbf{0})$ is shown in Fig. 6. An alternative expression for J_0 can be formulated in terms of the site-diagonal blocks of the Green functions $g^{\sigma}_{\mathbf{RR}}(z)$ which represents a sum rule to the quantities $J_{\mathbf{RR}'}$ and which serves as an independent check of accuracy.[20,21] Note that for systems with a ferromagnetic ground state, the parameter J_0 is proportional to a mean-field estimate of the Curie

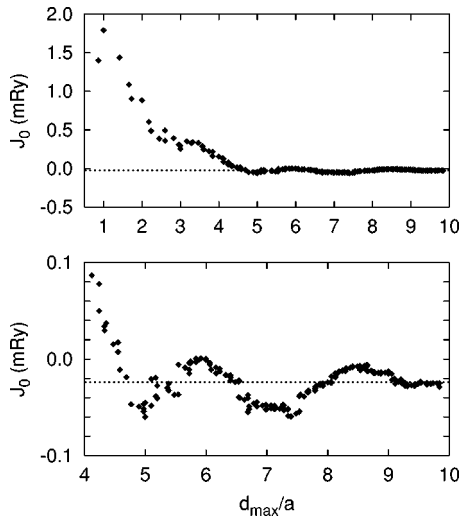

FIG. 6. The parameter $J_0 \equiv J(\mathbf{0})$ for bcc Eu as a function of the cutoff distance $d_{\max}$ used in the real-space summation in Eq. (3): the entire data set (upper panel) and the data for $d_{\max} > 4a$ (bottom panel). The dotted horizontal lines mark the exact value of J_0 obtained from a sum rule (Ref. 20).

temperature.[20,21] It is seen that the initial positive contribution to J_0 due to the first two neighboring shells is counteracted by the contribution of more distant sites, leading thus to a negligible resulting value $J_0 = -0.03 \pm 0.02$ mRy fully consistent with that from the sum rule, $J_0^{\mathrm{sr}} = -0.024 \pm 0.001$ mRy (the small error of the latter is due to a numerical BZ average[20,21]). Such a situation indicates again an instability of the FM state with respect to a more complicated spin structure.

C. Magnetic ground state

Determination of the ground state for the effective Heisenberg Hamiltonian, Eq. (1), is a difficult task in view of the highly dimensional manifold of *a priori* possible states as well as a number of qualitatively different spin structures encountered in RE-based systems.[14] Here we consider only spin spirals specified by a single $\mathbf{q}$ vector as

$$\overline{\mathbf{e}}_{\mathbf{R}} = [\sin(\mathbf{q}\cdot\mathbf{R}), 0, \cos(\mathbf{q}\cdot\mathbf{R})], \tag{4}$$

since the spin structure observed for bcc Eu at low temperatures belongs to this class.[23,24] The minimum of the Hamiltonian H_{eff} corresponds then to the maximum of the lattice Fourier transform $J(\mathbf{q})$, Eq. (3).

A scan over the whole BZ reveals that the absolute maximum of $J(\mathbf{q})$ (for the theoretical equilibrium Wigner-Seitz radius $s = 4.19$ a.u.) is obtained for a vector $\mathbf{q} = \mathbf{Q}$ inside the Γ-H line, namely at $\mathbf{Q} = (1.69, 0, 0)a^{-1}$; see Fig. 7. The magnitude of $\mathbf{Q}$ determines the angle ω between magnetic moments in the neighboring (100) atomic layers. In the present case, it is equal to $\omega = 48°$. Similar values were obtained for the experimental value of the Wigner-Seitz radius $s_{expt} = 4.238$ a.u., namely $\mathbf{Q} = (1.63, 0, 0)a^{-1}$, $\omega = 47°$ (see Fig. 7). Both data sets are in surprising agreement with experimental results which report the spin-spiral $\mathbf{q}$ vector inside the

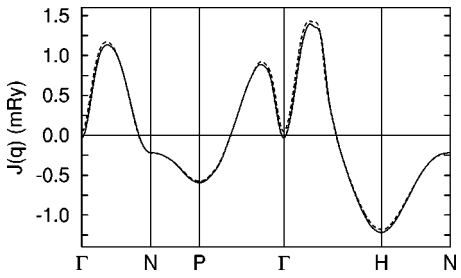

FIG. 7. The lattice Fourier transform $J(\mathbf{q})$ of the exchange interactions in bcc Eu along high-symmetry lines in the Brillouin zone calculated for a theoretical equilibrium lattice constant (full line) and for an experimental low-temperature lattice constant (dashed line).

Γ-H line and the angle per layer equal to $\omega_{expt} = 49°$ (Ref. 23) and $\omega_{expt} = 47.6 \pm 1.2°$ (Ref. 24).

D. The Néel temperature

The simplest estimate of the Néel temperature T_{N} of a spin spiral with a vector $\mathbf{Q}$ is based on a mean-field approximation (MFA) which leads to[14]

$$k_{\mathrm{B}} T_{\mathrm{N}}^{MFA} = \frac{2}{3} J(\mathbf{Q}), \tag{5}$$

where k_{B} is the Boltzmann constant, whereas an improved formula is provided by a random-phase approximation[37] (RPA)

$$(k_{\mathrm{B}} T_{\mathrm{N}}^{RPA})^{-1} = \frac{3}{4}\frac{1}{N}\sum_{\mathbf{q}} \{[J(\mathbf{Q}) - J(\mathbf{q})]^{-1} + [W(\mathbf{q},\mathbf{Q})]^{-1}\}, \tag{6}$$

where N denotes the number of primitive cells in the solid and

$$W(\mathbf{q},\mathbf{Q}) = J(\mathbf{Q}) - \frac{1}{2}J(\mathbf{q}+\mathbf{Q}) - \frac{1}{2}J(\mathbf{q}-\mathbf{Q}). \tag{7}$$

A derivation of Eq. (6) is sketched in the Appendix. It can be shown that $T_{\mathrm{N}}^{RPA} < T_{\mathrm{N}}^{MFA}$ in analogy to a relation for the approximative Curie temperatures of a ferromagnet.[21] The evaluation of T_{N}^{RPA} was based on the magnon Green functions[21] corresponding to the two terms in Eq. (6) and on a numerical procedure for analytic continuation of functions of a complex variable.[38]

The calculated values equal to $T_{\mathrm{N}}^{MFA} = 147$ K and $T_{\mathrm{N}}^{RPA} = 110$ K for the theoretical Wigner-Seitz radius ($s = 4.19$ a.u.), while for the experimental lattice ($s_{expt} = 4.238$ a.u.) values of $T_{\mathrm{N}}^{MFA} = 151$ K and $T_{\mathrm{N}}^{RPA} = 111$ K were obtained. Having in mind the approximative character of the electronic structure calculations as well as of Eq. (6), the RPA values are in reasonable agreement with the experimental value $T_{\mathrm{N}}^{expt} = 90.5 \pm 0.5$ K.[23,24]

The overestimation of the calculated Néel temperature with respect to the experiment can be partly assigned to assumed rigidity of the moment magnitudes. A recent theoret-

ical study of the magnon spectra of late RE metals (Gd through Tm) proves that a possible noncollinearity between the localized ($4f$) and itinerant (predominantly $5d$) moments leads to a softening of the magnon energies.[9] In the case of Gd, the restriction to collinear arrangements enhances the magnon energies by a factor of 1.5 in the upper part of the spectrum. However, the lower part of the spectrum, which is more important for a RPA estimation of the Curie temperature,[21] is less influenced. It can be expected that a similar mechanism applies for Eu, but its quantitative assessment remains beyond the scope of the present paper.

IV. CONCLUSIONS

We have shown that the simple open-core treatment of the $4f$ electrons in bcc Eu improves significantly the calculated equilibrium lattice constant as compared to the standard LSDA. This approach can hardly be considered a final solution to the problem of electron theory of rare-earth metals; however, it provides a sound basis for quantitative investigations of magnetic properties in terms of an effective classical Heisenberg Hamiltonian. We have demonstrated that the exchange interactions are long-ranged and oscillatory, which leads to a noncollinear magnetic ground state that is formed even in the presence of a dominating ferromagnetic interaction between the nearest neighbors on the bcc lattice. The knowledge of the exchange interactions in the real space ($J_{\mathbf{RR}'}$) enables an efficient search for a possible magnetic ground state by calculating their lattice Fourier transform $J(\mathbf{q})$ on a dense mesh of $\mathbf{q}$ vectors inside the Brillouin zone. The resulting $\mathbf{q}$ vector of the spin spiral as well as a RPA value of the Néel temperature are in good quantitative agreement with experimental data.

Similar agreement has been obtained using the present scheme also for ferromagnetic gadolinium.[39] We believe that the Heisenberg Hamiltonian with parameters derived from a self-consistent electronic structure[20,32] is a framework that might replace existing approaches to finite-temperature properties,[6,22] not only for elementary rare-earth metals but also for their alloys with other elements and intermetallics. The above approach represents an *ab initio* description of truly localized $4f$ magnetic moments coupled by itinerant *spd* electrons,[14] but it can also be modified in order to include effects of strong electron-electron correlations on a more profound level.[40]

ACKNOWLEDGMENTS

The authors acknowledge the support provided by the Grant Agency of the Czech Republic (No. 202/00/0122 and No. 106/02/0943), the Academy of Sciences of the Czech Republic (No. Z2041904), the Ministry of Education of the Czech Republic (No. MSM113200002), the Scientific and Technological Cooperation between Germany and the Czech Republic (No. TSR-013-98), and the RT Network ''Computational Magnetoelectronics'' (Contract No. HPRN-CT-2000-00143) of the European Commission.

APPENDIX: NÉEL TEMPERATURE IN THE RPA

The RPA for the classical Heisenberg Hamiltonian, Eq. (1), with a spin-spiral ground state, Eq. (4), can be developed in analogy to the case of a ferromagnet.[37,41] First, we apply local rotations around the y axis in order to introduce local frames such that the unit vectors $\overline{\mathbf{e}_\mathbf{R}}$ of the spin spiral, Eq. (4), point along the local z axes. The components $(\xi_\mathbf{R}, \eta_\mathbf{R}, \zeta_\mathbf{R})$ of a general unit vector $\mathbf{e}_\mathbf{R}$ in the global frame are then expressed as

$$\xi_\mathbf{R} = \cos(\mathbf{Q}\cdot\mathbf{R})x_\mathbf{R} + \sin(\mathbf{Q}\cdot\mathbf{R})z_\mathbf{R},$$

$$\eta_\mathbf{R} = y_\mathbf{R},$$

$$\zeta_\mathbf{R} = -\sin(\mathbf{Q}\cdot\mathbf{R})x_\mathbf{R} + \cos(\mathbf{Q}\cdot\mathbf{R})z_\mathbf{R}, \tag{A1}$$

where $\mathbf{Q}$ is the spin-spiral wave vector and $(x_\mathbf{R}, y_\mathbf{R}, z_\mathbf{R})$ are components of the vector $\mathbf{e}_\mathbf{R}$ in its local frame. The spin-spiral state below the Néel temperature is featured by $\langle x_\mathbf{R}\rangle = \langle y_\mathbf{R}\rangle = 0$ and $\langle z_\mathbf{R}\rangle \neq 0$, where $\langle \ldots \rangle$ denotes the statistical (thermodynamic) average. The original isotropic Heisenberg Hamiltonian with a symmetry-breaking external magnetic field b can be written in the new variables as

$$H_{\mathrm{eff}} = H_1 + H_2, \tag{A2}$$

where H_1 is an anisotropic Heisenberg Hamiltonian

$$H_1 = -\sum_{\mathbf{RR}'} \left(K_{\mathbf{RR}'}x_\mathbf{R}x_{\mathbf{R}'} + L_{\mathbf{RR}'}y_\mathbf{R}y_{\mathbf{R}'} + M_{\mathbf{RR}'}z_\mathbf{R}z_{\mathbf{R}'}\right) - b\sum_\mathbf{R} z_\mathbf{R}, \tag{A3}$$

while H_2 collects all remaining terms, namely,

$$H_2 = 2\sum_{\mathbf{RR}'} N_{\mathbf{RR}'}x_\mathbf{R}z_{\mathbf{R}'}. \tag{A4}$$

The pair interactions in Eqs. (A3) and (A4) are given by

$$K_{\mathbf{RR}'} = M_{\mathbf{RR}'} = J_{\mathbf{RR}'}\cos[\mathbf{Q}\cdot(\mathbf{R}-\mathbf{R}')],$$

$$L_{\mathbf{RR}'} = J_{\mathbf{RR}'},$$

$$N_{\mathbf{RR}'} = J_{\mathbf{RR}'}\sin[\mathbf{Q}\cdot(\mathbf{R}-\mathbf{R}')]. \tag{A5}$$

They exhibit full translation invariance provided the original interactions $J_{\mathbf{RR}'}$ possess the same property.

Second, magnons for the resulting Hamiltonian in the transformed variables are studied.[37] Since the term H_2 with parameters $N_{\mathbf{RR}'}$ given by Eq. (A5) does not contribute to zero-temperature magnons, it is omitted here also for finite temperatures. Application of the method of equation of motion for the two-time retarded Green functions to the anisotropic Heisenberg Hamiltonian H_1 and a RPA-decoupling[37] lead to a transition temperature

$$(k_B T_{\mathrm{tr}}^{RPA})^{-1} = \frac{3}{4}\frac{1}{N}\sum_{\mathbf{q}} \{[M(\mathbf{0}) - K(\mathbf{q})]^{-1} + [M(\mathbf{0}) - L(\mathbf{q})]^{-1}\}, \quad \text{(A6)}$$

where $K(\mathbf{q})$, $L(\mathbf{q})$, $M(\mathbf{q})$ refer to the lattice Fourier transforms, cf. Eq. (3), of the corresponding pair interactions in Eq. (A3). In the case of a spin spiral, Eq. (A5), they are given by $L(\mathbf{q}) = J(\mathbf{q})$ and

$$K(\mathbf{q}) = M(\mathbf{q}) = \frac{1}{2}[J(\mathbf{q}+\mathbf{Q}) + J(\mathbf{q}-\mathbf{Q})]. \quad \text{(A7)}$$

Substitution of these relations into Eq. (A6) yields the final formula for the Néel temperature, Eq. (6).

*Email address: turek@ipm.cz

[1] P. Hohenberg and W. Kohn, Phys. Rev. **136**, B864 (1964).
[2] H. Eschrig, *The Fundamentals of Density Functional Theory* (Teubner, Leipzig, 1996).
[3] W. Kohn and L.J. Sham, Phys. Rev. **140**, A1133 (1965).
[4] U. von Barth and L. Hedin, J. Phys. C **5**, 1629 (1972).
[5] J.P. Perdew and Y. Wang, Phys. Rev. B **33**, 8800 (1986).
[6] M. Richter, J. Phys. D **31**, 1017 (1998).
[7] M.S.S. Brooks, L. Nordström, and B. Johansson, J. Phys.: Condens. Matter **3**, 2357 (1991).
[8] R. Schumann, M. Richter, L. Steinbeck, and H. Eschrig, Phys. Rev. B **52**, 8801 (1995).
[9] A.Y. Perlov, S.V. Halilov, and H. Eschrig, Phys. Rev. B **61**, 4070 (2000).
[10] J.O. Dimmock and A.J. Freeman, Phys. Rev. Lett. **13**, 750 (1964).
[11] S.C. Keeton and T.L. Loucks, Phys. Rev. **146**, 429 (1966).
[12] A.B. Shick, A.I. Liechtenstein, and W.E. Pickett, Phys. Rev. B **60**, 10763 (1999).
[13] P. Strange, A. Svane, W.M. Temmerman, Z. Szotek, and H. Winter, Nature (London) **399**, 756 (1999).
[14] J. Jensen and A.R. Mackintosh, *Rare Earth Magnetism* (Clarendon, Oxford, 1991).
[15] L. Nordström and A. Mavromaras, Europhys. Lett. **49**, 775 (2000).
[16] G. Bihlmayer, P. Kurz, and S. Blügel (unpublished).
[17] B.L. Gyorffy, A.J. Pindor, J. Staunton, G.M. Stocks, and H. Winter, J. Phys. F: Met. Phys. **15**, 1337 (1985).
[18] V.P. Antropov, B.N. Harmon, and A.N. Smirnov, J. Magn. Magn. Mater. **200**, 148 (1999).
[19] J.B. Staunton and B.L. Gyorffy, Phys. Rev. Lett. **69**, 371 (1992).
[20] A.I. Liechtenstein, M.I. Katsnelson, V.P. Antropov, and V.A. Gubanov, J. Magn. Magn. Mater. **67**, 65 (1987).
[21] M. Pajda, J. Kudrnovský, I. Turek, V. Drchal, and P. Bruno, Phys. Rev. B **64**, 174402 (2001).
[22] M.S.S. Brooks and B. Johansson, in *Handbook of Magnetic Materials*, edited by K.H.J. Buschow (North-Holland, Amsterdam, 1993), Vol. 7, Chap. 3, p. 139.
[23] N.G. Nereson, C.E. Olsen, and G.P. Arnold, Phys. Rev. **135**, A176 (1964).
[24] A.H. Millhouse and K.A. McEwen, Solid State Commun. **13**, 339 (1973).
[25] O.K. Andersen and O. Jepsen, Phys. Rev. Lett. **53**, 2571 (1984).
[26] I. Turek, V. Drchal, J. Kudrnovský, M. Šob, and P. Weinberger, *Electronic Structure of Disordered Alloys, Surfaces and Interfaces* (Kluwer, Boston, 1997).
[27] S.H. Vosko, L. Wilk, and M. Nusair, Can. J. Phys. **58**, 1200 (1980).
[28] O.K. Andersen, Phys. Rev. B **12**, 3060 (1975).
[29] E. Wimmer, H. Krakauer, M. Weinert, and A.J. Freeman, Phys. Rev. B **24**, 864 (1981).
[30] P. Blaha, K. Schwarz, and J. Luitz, WIEN97, Vienna University of Technology, 1997.
[31] P. Kurz, G. Bihlmayer, and S. Blügel, J. Phys.: Condens. Matter **14**, 6353 (2002).
[32] A. Oswald, R. Zeller, P.J. Braspenning, and P.H. Dederichs, J. Phys. F: Met. Phys. **15**, 193 (1985).
[33] M. Heinemann and W.M. Temmerman, Phys. Rev. B **49**, 4348 (1994).
[34] O. Eriksson, R. Ahuja, A. Ormeci, J. Trygg, O. Hjortstam, P. Söderlind, B. Johansson, and J.M. Wills, Phys. Rev. B **52**, 4420 (1995).
[35] J.F. Janak, V.L. Moruzzi, and A.R. Williams, Phys. Rev. B **12**, 1257 (1975).
[36] M.S.S. Brooks, B. Johansson, and H.L. Skriver, in *Handbook on the Physics and Chemistry of the Actinides*, edited by A.J. Freeman and G.H. Lander (North-Holland, Amsterdam, 1985), Vol. 1, Chap. 3, p. 153.
[37] S.V. Tyablikov, *Methods of Quantum Theory of Magnetism* (Plenum Press, New York, 1967).
[38] K.C. Hass, B. Velický, and H. Ehrenreich, Phys. Rev. B **29**, 3697 (1984).
[39] I. Turek, J. Kudrnovský, G. Bihlmayer, and S. Blügel, J. Phys.: Condens. Matter **15**, 2771 (2003).
[40] M.I. Katsnelson and A.I. Lichtenstein, Phys. Rev. B **61**, 8906 (2000).
[41] C.S. Wang, R.E. Prange, and V. Korenman, Phys. Rev. B **25**, 5766 (1982).